Environmental Fluid Mechanics (2005) 5: 357–372
DOI 10.1007/s10652-004-7301-4

High Spatial and Temporal Variability of Dry Deposition in a Coastal Region

MARK ŽAGAR*, GUNILLA SVENSSON and MICHAEL TJERNSTRÖM
Department of Meteorology, Stockholm University, S-10691 Stockholm, Sweden

Received 14 April 2004; accepted in revised form 1 December 2004

Abstract. A real meteorological situation characterized by strong spatial and temporal variability of the meteorological fields in a coastal region of eastern Denmark is examined in view of the transport of a passive tracer and dry deposition. Model simulations using a full mesoscale NWP model (COAMPS^{TM}) at different horizontal resolutions are performed. A realistic simulation showed that the differences in the amount of dry deposited matter can reach one order of magnitude and larger, during the period of one afternoon, depending on the model horizontal resolution. In addition, the results of an idealized experiment with straight coastline indicate that the horizontal model resolution alone is responsible for most of the differences. This study confirms the importance of high spatial and temporal resolution modelling for environmental applications.

Key words: air-sea interaction, dry deposition, coastal modeling, Kattegat, sea-breeze

1. Introduction

Repeating occurrences of harmful algae blooms and their economic consequences have recently received scientific interest in the area of the Kattegat strait [1], Figure 1. The project named MEAD (Marine Effects of Atmospheric Deposition; see [2]) was organized to concentrate on this particular issue. In summer time, when the riverine input of the nutrients is small, the atmospheric deposition is expected to play an important role in supplying the nutrients, needed for growth of phytoplankton and, in extreme events, its blooms. The abundant sources of ammonia at Jutland (northern Denmark) combined with prevailing western winds present favourable conditions for nutrification of the Kattegat. In order to study such a particular issue one should first recognize the general coastal problem, which is high spatial and temporal variability of the atmosphere.

Due to relatively fast rates of deposition of ammonia, large gradients in the local dry deposition in the vicinity of sources are known to occur

*Corresponding author, E-mail: mark@misu.su.se

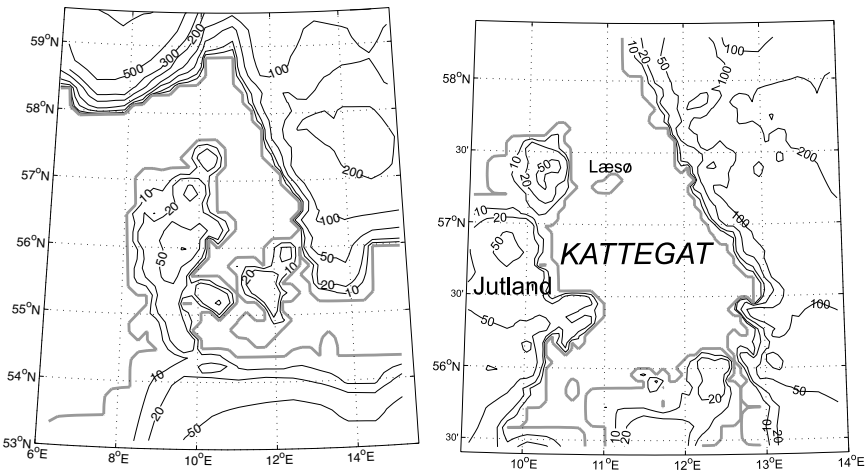

Figure 1. The terrain topography as seen in the model at the horizontal grid spacing 15 km (left) and 5 km (right). The coastline is drawn with the thick line and the terrain altitude is drawn with thin lines at 10, 20, 50, 100, 200, 300, 500 and 1000 m.

[3,4]. In spite of this, even large scale transport and deposition models have been regarded as successful in reproducing the observed state (e.g. [5]). The reason for such conclusions is that the observed distribution of the dry deposited ammonia is supported by too coarse (in both time and space) a network of measurements. In the same study Hasager *et al.* [5] concluded, on the basis of the results from a 30 km grid spacing model, that the nitrogen input to the marine surface by dry deposition is insignificant for algal blooms in the area of the Kattegat strait. However, the present study indicates that local deposition events of much larger amplitude can occur under certain situations, for example when the sea-breeze significantly modifies the large-scale flow. As Schlunzen and Pahl have shown in their numerical study [6], the development of the sea-breeze strongly affects the three dimensional distribution of a tracer gas and the dry deposition velocity. The combined effect leads to a complex distribution of dry deposited gas over a life cycle of the sea-breeze circulation, one half of a day. Also other features than the sea-breeze in the wind field in vicinity of the coast, like friction induced convergence, or sudden change in the surface temperature, as two examples, may have a significant effect on dry deposition. Žagar *et al.* [7] attempted to systematically describe variations in the surface turbulent momentum flux (which can serve as a proxy for deposition velocity) near the coast for off-shore and on-shore wind situations. While those wind features that result from the effect of friction and topography at the small-scale can be efficiently downscaled using for example a dynamic adaptation approach [8], the thermally induced local circulations

as the sea-breeze can only be modelled by an appropriate and complete high resolution numerical model.

In this paper we attempt to evaluate, qualitatively and quantitatively, the impact of the horizontal resolution in a mesoscale NWP model (COAMPS™) with treatment of the tracer gas. The meteorological part of the model simulation for the given situation is validated here through comparison with observations. The model itself is described in Section 2. The significant features of the meteorological situation, in particular the weak sea-breeze that is only reproduced in the high resolution model, are discussed in Section 3. The results of modelling the tracer transport and dry deposition are presented in Section 4 for a real case over the Kattegat, and in Section 5 for an idealized experiment where the only difference between the two simulations is the horizontal model resolution. Finally, the most important conclusions are assembled in Section 6.

2. The Model

The model's representation of the shape of the coast and the topography over the area of interest, the Kattegat strait between Denmark and Sweden, in two different horizontal resolutions (15 km and 5 km grid spacing), is shown in Figure 1. One important difference between the two representations is the presence of the Læsø island in the high resolution model only. The effect of Læsø on the spreading and deposition of a passive tracer gas will be demonstrated in the following sections.

The numerical simulations were performed with the COAMPS™ version 2 atmospheric model, developed at the US Naval Research Lab, Monterey, CA [9]. It is a primitive equation compressible Boussinesq model with terrain-following vertical coordinate. The turbulent kinetic energy is a prognostic variable and provides the input to the 2.5 level turbulence closure [10]. The diabatic part of the model includes explicit moist physics computation [11] and at very high resolution it effectively becomes a cloud-resolving model. Subgrid convection at lower resolutions (greater than 10 km grid spacing) is parameterized using a version of the Kain-Fritsch mass-flux scheme [12]. Transfer and absorption of radiation is treated as in [13]. The ground surface temperature is computed taking into account different land classes with pre-defined albedo (for snow-free surface), and the soil moisture is computed using a single layer bucket model. The initial and lateral boundary conditions in our simulation were provided by ECMWF analyses using Davies relaxation scheme [14]. Consecutive static nesting was used in the simulations. The horizontal resolution of every nest was three times higher than that of the parent nest. The vertical resolution did not change between the nests; 40 levels were used in the simulations. The levels were very densely distributed in the planetary boundary layer (13 levels within

lowest 1 km, 5 within lowest 100 m, the two lowest levels at 1 m and 5 m above surface).

The tracer model (one of the modules in COAMPS™) in our simulations consists of the source, transport and dry deposition of a tracer gas. The advection scheme used is the Bott's forward-in-time, positive-definite, area-preserving flux-form algorithm [15,16]. The emitted gaseous matter is instantly mixed throughout the lowest model layer. This is an acceptable assumption for this simulation, focused on the evolution during the afternoon. Otherwise, especially when the surface layer is stable, one should verify that the used model satisfies the criteria in [17] concerning the dry deposition near the source itself. Ammonia in our simulations is considered as a true tracer gas, meaning that it is not chemically active and is not converted into ammonium aerosol particles.

The flux of the dry deposition of ammonia to the surface, F, is computed as:

$$F = v_{\mathrm{d}} C(z_{\mathrm{r}}), \tag{1}$$

where v_{d} is the deposition velocity and $C(z_{\mathrm{r}})$ is the concentration at the reference height z_{r}. The deposition velocity is represented by resistances:

$$v_{\mathrm{d}} = \frac{1}{r_{\mathrm{a}} + r_{\mathrm{b}} + r_{\mathrm{c}}}, \tag{2}$$

where r_{a}, r_{b} and r_{c} are the aerodynamic, quasi-laminar sub-layer and canopy resistances, respectively. The aerodynamic resistance is a function of wind speed, surface properties and atmospheric stability [18]. The quasi-laminar surface boundary layer resistance is associated with transfer through the quasi-laminar layer in contact with the surface [18]. This resistance is strongly influenced by the diffusivity of the material being transferred. The canopy resistance is for simplicity taken as a constant value, instead of using a canopy model. The values for ammonia (NH_3), used in the simulation are $r_{\mathrm{c}} = 600$ over land, assuming low vegetation and $r_{\mathrm{c}} = 240$ over water [3].

3. The Meteorological Situation

To demonstrate to which extent the local influences can modify the atmospheric circulations we have chosen an episode with weakly expressed sea-breeze circulation at the eastern coast of Jutland. When the forcing is weak, as it is the case with the incoming solar radiation at these relatively high latitudes, its effects are subtle and therefore the modelling approach has to be more accurate, implying a sufficiently high spatial resolution.

During the period between 12 August and 14 August 2000, a high-pressure rigde strengthened somewhat over the central and northern

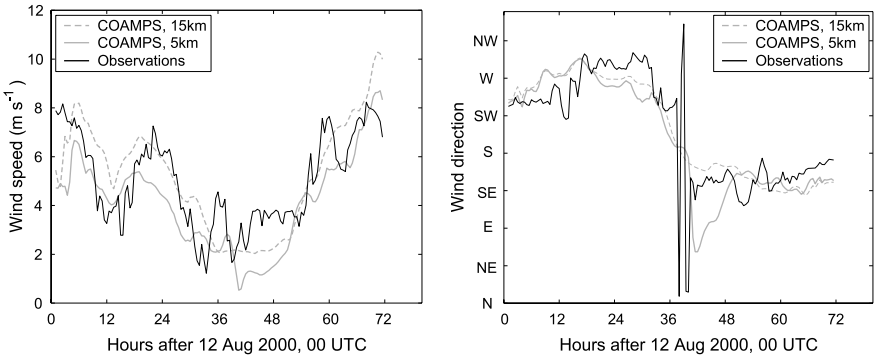

Figure 2. The observed (black line) and COAMPS™ simulated (full and dashed gray lines) wind speed and direction at the western tip of the Læsø island or the corresponding point in the 15 km model. Values every half an hour between 12 August, 00 UTC and 15 August, 00 UTC are plotted.

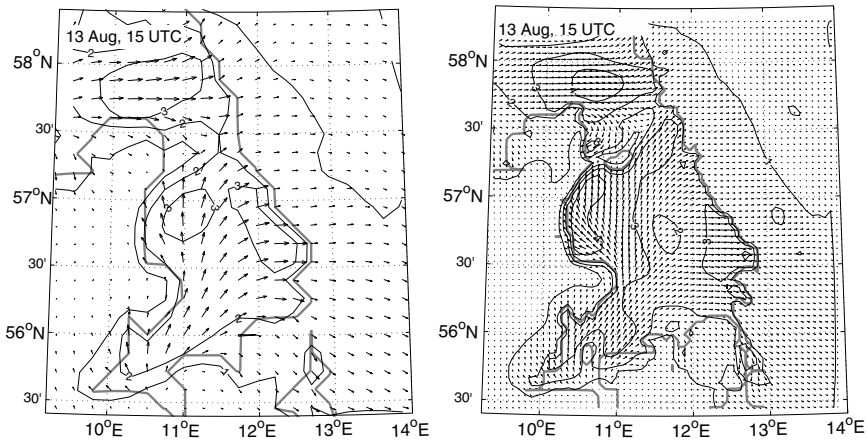

Figure 3. 13 August 2000, 15 UTC: the wind field at 5 m above ground modelled by COAMPS™ at 15 km grid spacing (left) and 5 km grid spacing (right). Wind velocity is shown by isolines every 1 m/s.

Europe. As a consequence the wind direction shifted from WNW towards WSW in the free troposphere above northern Kattegat. At the surface, however, the topography and the weak daytime thermal low over the northern Denmark caused a much more complex evolution of the wind field. Figure 2 shows the observed and the simulated wind evolution at the western tip of the Læsø island, during the three days. The model was able to reproduce the main wind features in both speed and direction at both resolutions (Figure 3), but naturally there are more small scale details present in the 5 km simulation. During the first 36 h of the simulation, which started on 12 August, 00 UTC, models with 15 and 5 km grid spacing do

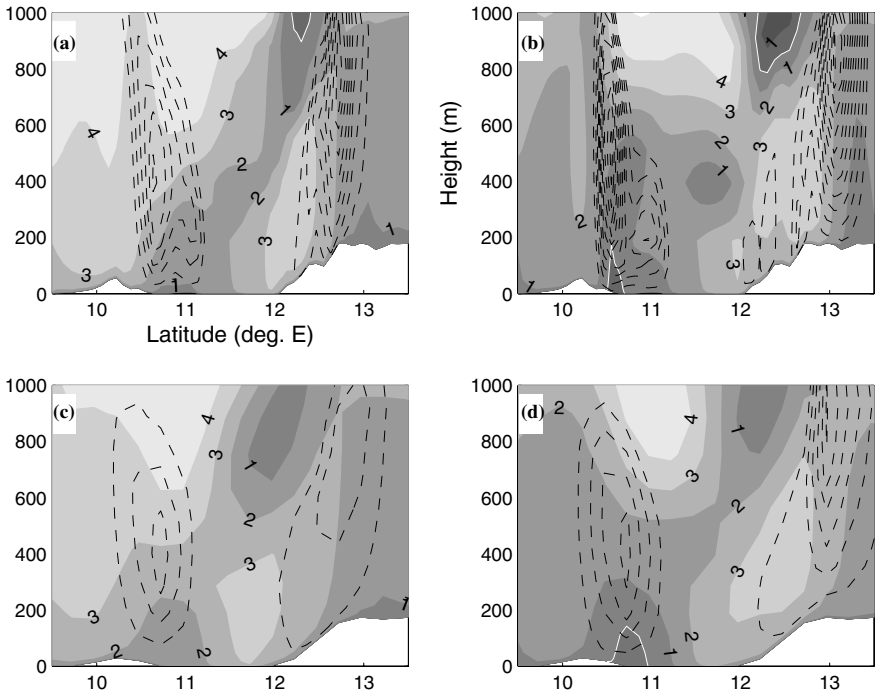

Figure 4. Vertical cross-sections across the Kattegat at the latitude of the western tip of Læsø island. The 5 km model (a, b) and 15 km model (c, d) results are shown on 13 August 2000 at 12 UTC (a, c) and 15 UTC (b, d). Shades represent the u-component of the horizontal wind in m/s and the white isoline in b and d limits the zero value. Upward vertical velocity is denoted with dashed contours in 1 cm/s intervals.

not behave very differently. Later on, the small-scale features become more influential to the wind pattern, not least due to the presence of the Læsø island. Therefore the shift in the wind direction from SW to SE with temporary excursion to N between the 36th and 42nd hour seems to be more realistically described in the high resolution model (Figure 2). In particular the relative drop in the wind speed around the time 40 h and correspondent sharp change in the wind direction are most noteworthy and can be explained by careful examination of the dynamics in the 5 km model. A lee wake behind the sharp turn of the coast at the northern tip of Jutland in combination with the sea-breeze, caused a significant easterly wind at the coast of Jutland, north of the Læsø island. This has in turn created a sharp wind front, whose spatial oscillations caused the observed northerly wind spikes at Læsø. According to the model this wind front has not passed Læsø but remained instead quasi stationary north of the island and dissolved when the sea-breeze died out later in the day. The observations from

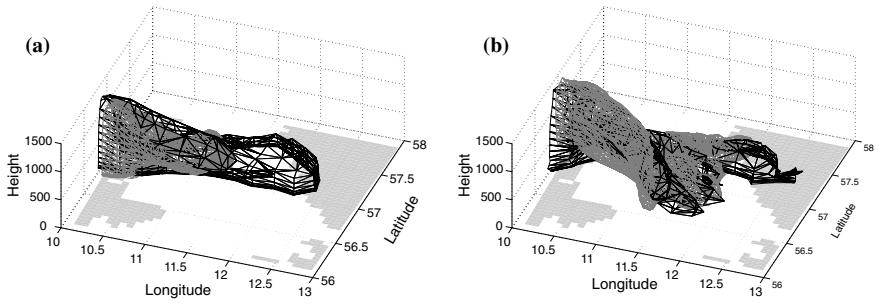

Figure 5. 13 August 2000, 12 UTC (a) and 18 UTC (b). The concentration of ammonia over the Kattegat region, modelled by the model with 5 km grid spacing (gray colour) and 15 km grid spacing (black colour). The isosurface bounding the significant concentration (1 mg/m^3) is plotted.

Læsø, though sparse, confirm such an evolution of the wind conditions on this day. Figure 4 shows the vertical cross-sections across the Kattegat, exactly over the tip of Læsø (or model equivalent). Evidently the situation looks quite similar at both model resolutions at 12 UTC, i.e. before the sea-breeze developed. Also at 15 UTC the differences are small, except for an additional u-wind component minimum at around 400 m above the eastern Kattegat in the 5 km model. Some easterly wind is present close to the surface near the coast of Jutland at both model resolutions. However, the vertical wind pattern, which exhibits a local maximum at around 200 m at longitude 11°, where Læsø is, indicates some low-level wind convergence in the 5 km model, but not in the 15 km one. This appears to be the same signal as seen in the horizontal wind pattern, connected to the wind convergence front, discussed earlier. Later, in Section 4, we show how important these subtle differences in the point-to-point comparison with observations are as regards the dry deposition of a tracer gas.

4. Tracer Transport and Dry Deposition

It follows from (2) that in absence of any conversion processes being applied to the tracer in the model, the dry deposition is exclusively defined by the meteorological conditions. Since the two models that differ only in the horizontal resolution exhibit significant differences in the modelled wind field – as demonstrated in the previous section – it is expected that similar differences will also be present in the concentration and deposition fields.

The source of the ammonia in the simulations is located at the surface over a circular region with radius of 50 km, centered over the northern Jutland. The emission is constant in time, 1600 mg/m^2/day in the centre and diminishing as a cosinus function towards the edges of the circle. The

source location corresponds to the area of a local maximum in [17] (their Figure 5). The emission was chosen so that the average concentration of ammonia in the surface layer, on the daily basis of the given day (13 August 2000), is around two to three times larger than the average value, reaching 3.9 μg/m^3, given in [17]. The results of our simulations should, however, not be regarded by the absolute values of ammonia concentrations, due to rather arbitrarily chosen emission scenario.

The impact of the model resolution on the three-dimensional field of tracer concentration is clearly seen in the middle of the day, at 12 UTC (Figure 5a). The tracer gas spreads much further eastward in the 15 km model than in the 5 km model, where any significant tracer concentration downwind from the Læsø island is absent. Because the vertical extent of the tracer plume is low, only some 600 m high above the strip of sea east of Jutland in 15 km model but even less in the 5 km model, the convective boundary layer (CBL) above the Læsø island effectively prevents the tracer gas from spreading further east. Moreover, it appears that some of the tracer has been trapped inside the CBL above the island. Of course, the three-dimensional wind field is primarily important in this context since it is the convergence at the wind front that causes the plume of the tracer gas to be so narrow in the first place. At 18 UTC, however, both 15 km and 5 km models exhibit similar picture of the spreading of the tracer gas (Figure 5b).

The wind is not only important for the three-dimensional distribution of the tracer gas. Also the surface turbulent momentum flux and, as a consequence, r_a, favour dry deposition where the wind is stronger. Another variable that governs the surface turbulent momentum flux is the static stability, or the temperature lapse rate above the sea surface. In the absence

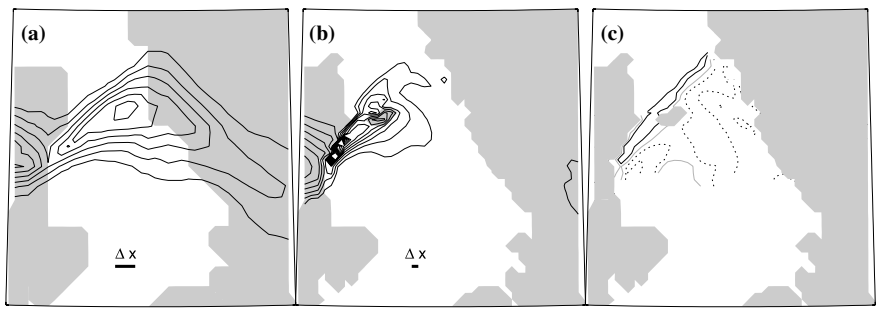

Figure 6. 13 August 2000, 13 UTC. 1 h accumulated dry deposited ammonia in (a) the model with 15 km grid spacing, (b) 5 km grid spacing. Interval between the isolines is 2 mg/m^2. (c) The ratio between the higher and lower resolution model. Full black lines in (c) (and also in Figures 7–10, c) denote regions with values above 2, 5, 10; dashed lines denote regions with values below 0.5, 0.2, 0.1; equal values are represented by the full gray line.

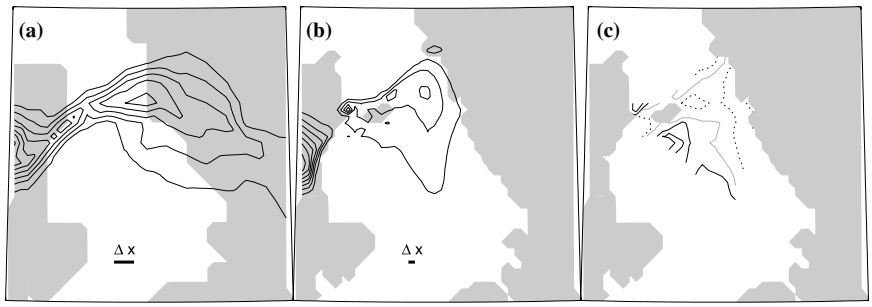

Figure 7. As Figure 6 only for 16 UTC.

of the sea-breeze, as in the 15 km model, the warm air from above Jutland is advected over the cold sea surface causing a very stably stratified lowest layer and effectively decoupling the advected polluted air from the sea surface thus inhibiting dry deposition. Instead, the tracer gas is brought inside the developing internal marine boundary layer by entrainment from above, which is a considerably slower process than horizontal advection. Figure 6a illustrates this by showing the minimum of hourly dry deposition between 12 and 13 UTC in the coastal waters immediately to the east of Jutland, although the concentration of the tracer just above the surface layer exhibits a maximum value there, for all the grid points above the sea. In contrast, the 5 km model (Figure 6b) shows very high dry deposition during this time near the coast of Jutland in a maximum extending towards the north-east, up to the Læsø island. At the onset of the sea-breeze, the surface wind off-shore of Jutland, southeast of Læsø, first began to turn from SW direction into the SE direction thus keeping the tracer near the coast and pushing it towards the north, allowing enough time for the tracer to deposit. As a result, the hourly amount of dry deposited tracer near the coast of Jutland is about two times larger in the 5 km model, compared with the 15 km model. At the same time the deposition east of Læsø is up to 10 times larger in the 15 km model. Later, at 15 UTC, with the fully developed sea-breeze in the 5 km model (Figure 7b) the sea-breeze cell in its on-shore part is obviously free of ammonia and there is no dry deposition to the belt of the sea near the coast of Jutland. It can not be stated with sufficient confidence whether the dry deposition around Læsø is due to remaining ammonia in the marine air from earlier, or due to entrainment from above. However, in the 15 km model (Figure 7a) the change from three hours earlier is not so evident. The only thing worth mentioning is the somewhat increased dry deposition near the coast due to the same mechanisms, only weaker, than those that occurred in the 5 km model three hours earlier. Still, the amount of the tracer deposited to the eastern part of the Kattegat is over twice as large in the 15 km model, as

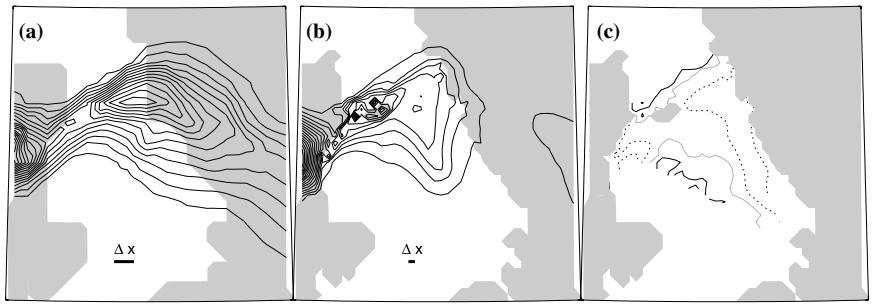

Figure 8. As Figure 6 only for 18 UTC. 6 h accumulation; interval between the isolines is 5 mg/m^2.

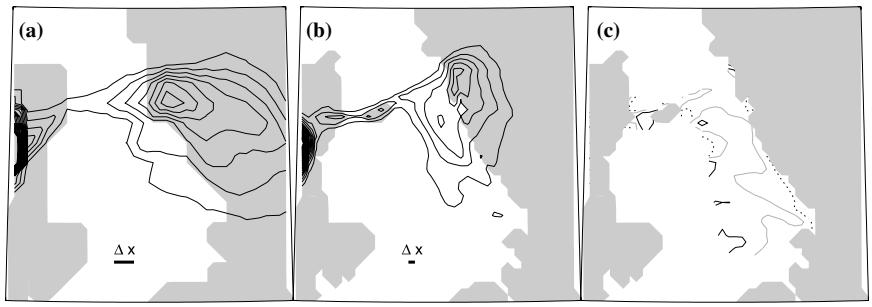

Figure 9. As Figure 6 only for 21 UTC. 3 h accumulation; interval between the isolines is 5 mg/m^2.

compared to the 5 km one (Figure 7c). Clearly, the evolution during the whole afternoon is consistently indicating that the impact of the horizontal model resolution (and the Læsø island) to the dry deposition is primarily seen in the amount deposited to the sea surface east of Læsø. The maximum accumulated 6 h dry deposited tracer (Figure 8) in the eastern Kattegat is 15 mg/m^2 versus 60 mg/m^2 in the 5 km and 15 km model, respectively, producing the ratio of four at nearly identical geographical location. On the other hand, the difference at the coastal waters near Jutland is much smaller, reaching the ratio of two (25 mg/m^2 versus 50 mg/m^2) in favour of the 5 km model and only at one isolated location. The situation in the early evening, between 18 UTC and 21 UTC does evidently not pose any significant resolution-dependent problems for the numerical model. The 3 h accumulation of dry deposited tracer gas at both resolutions, 5 km and 15 km, is very similar (Figure 9). In Figure 10 the 12 h dry deposition at both model resolutions is plotted, together with the ratio of the two. Again, the most obvious difference concerns the maximum of accumulated deposited tracer which is located in the eastern Kattegat in the 15 km model, while another maximum occurs between Jutland and Læsø in the 5 km model.

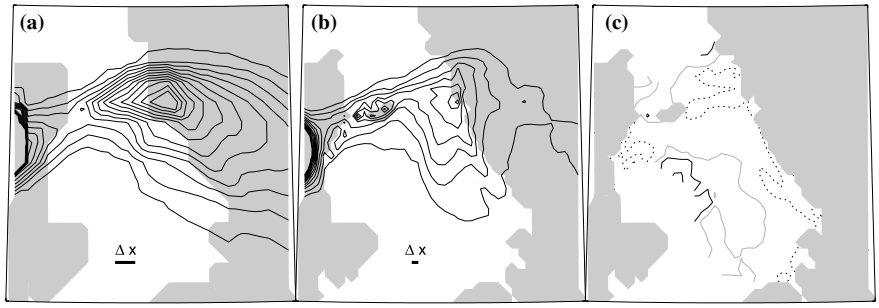

Figure 10. As Figure 6 only for 14 August, 00 UTC. 12 h accumulation; interval between the isolines is 10 mg/m^2.

Table I. The amounts of accumulated dry deposited tracer (mg/m^2) in the simulations of the 13 August 2000.

	12–13	15–16	12–18	18–21	12–24
15 km, E	12	10	60	20	110
15 km, W	10	8	35	5	30
5 km, E	2	6	20	20	60
5 km, W	>30	8	50	10	80

The maxima from two different model resolutions are shown separately for the eastern and western Kattegat (15 km, E, 15 km, W, 5 km, E and 5 km, W) and for different time intervals (top row in the table).

Table I summarizes the differences between the high-resolution and the low-resolution simulation for this real meteorological situation with simplified tracer modelling. The time intervals presented in this table are the same as in the Figures 6–10, and are chosen so that they cover different regimes: the onset of the sea-breeze (12–13 UTC), a developed sea-breeze (15–16 UTC), a whole afternoon (12–18 UTC), the evening transition (18–21 UTC) and the complete event (12–24 UTC).

It may appear, looking at the Figures 6–10, that the different distribution of the dry deposited tracer to the marine surface is the result of several subtle differences in the model at two resolutions and that the results from the low-resolution experiment may at least be used for estimating the rough limits of the actual values. However, the temporal variability of the hourly values of dry deposition (Figure 11) and the different location of the deposition means (Figure 12) indicate a danger that the literal interpretation of the low-resolution model could be fundamentally in error. Should, in a hypothetical application, the local deposition maxima be estimated from the 15 km model's variability (Figure 11c) and mean value (Figure

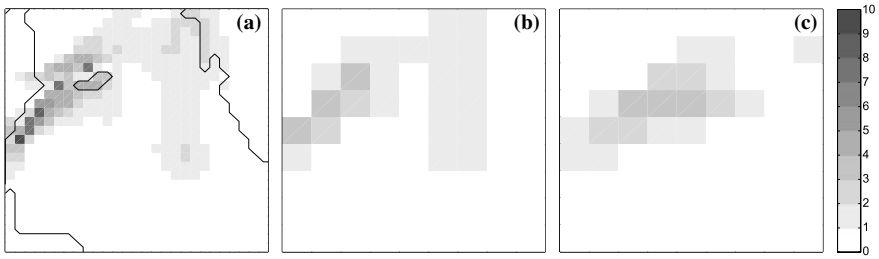

Figure 11. The standard deviation of the hourly accumulations of dry deposited ammonia in mg/m^2 between 12 and 18 UTC in (a) the 5 km model, (b) the 5 km model upscaled to 15 km grid and (c) the 15 km model. Note that the upscaling (b) is performed on the hourly values and the standard deviation is computed from the upscaled values.

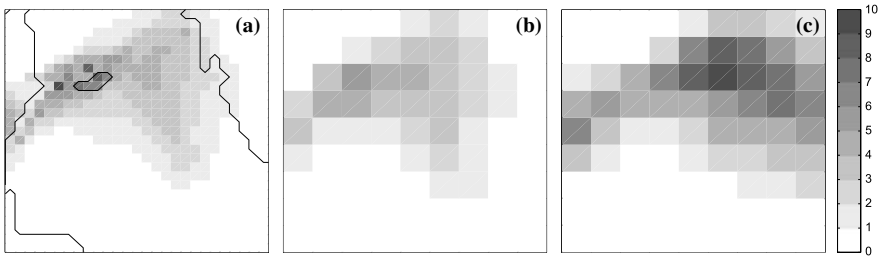

Figure 12. Mean 1 h accumulated dry deposited ammonia in mg/m^2 between 12 and 18 UTC on 13 August in (a) the 5 km model, (b) the 5 km model upscaled to 15 km grid and (c) the 15 km model.

12c), the potential area where high deposition can be expected is going to be located at the wrong place, i.e. in the eastern Kattegat and, judging by the relatively low variability, with a considerable confidence too. Nevertheless, Figure 11b and c show that the highest variability in the more detailed 5 km model is located along the coast of Jutland, and not in the middle of the Kattegat as in the 15 km model. The reason for the high variability in the 5 km simulation is mainly the strong deposition at the onset of the sea-breeze. In the 15 km simulation it is the off shore entrainment of the ammonia from the elevated plume into the marine boundary layer which causes the maximum of the dry deposition to shift along the downwind direction. This again shows that a low-resolution model is not necessarily just a somewhat less accurate version of the high-resolution one, but that it's result may contain grave systematic, physically grounded errors. Some of them are discussed in the following section.

5. Idealized Simulation

In a simulation with the realistic model topography it is impossible to separate the causes from their effects in a linear fashion. In our case we ask whether the locations of increased dry deposition are determined by the three-dimensional distribution of the tracer concentration, or rather by the deposition velocity. While it is obvious that both of them have to satisfy certain criteria in order to produce a deposition event, they are not equally revealing from the numerical modelling perspective. The deposition velocity has a local character and can be diagnosed if the wind speed and static stability (combined in surface wind stress) are known. The concentration field, on the other hand, is subjected to spatially and temporally integrated inaccuracies of the applied numerical model.

In order to gain some further understanding, we constructed an idealized numerical experiment, where the only difference between the two simulations is the horizontal model grid distance, 15 km and 5 km. The coast is a straight line in south–north direction, with land to the west. Large scale meteorological conditions correspond to those from the real case of 13 August 2000, with the WNW wind of about 5 m/s aloft and mostly clear weather.

Figure 13 shows the hourly accumulated dry deposition at 16 UTC and can be compared with Figure 7. Similar to the real case, the sea-breeze cell is not complete. There is some on-shore component in the wind near the surface but the marine air does not propagate inland and convergence occurs along the coast, on the seaward side. This general feature is present regardless of the model resolution. The convergence is mainly limited to the first off-shore grid points in both simulations. However, the wind stress is approximately three times stronger in the 5 km simulation, and also closer to the coast, around 10 km off-shore as opposed to around 30 km off-shore in the 15 km simulation. The horizontal extent of the sea-breeze circulation is similar in both simulations, 30–45 km. Figure 14 shows the vertical cross section of the tracer concentration in both runs at 15 UTC,

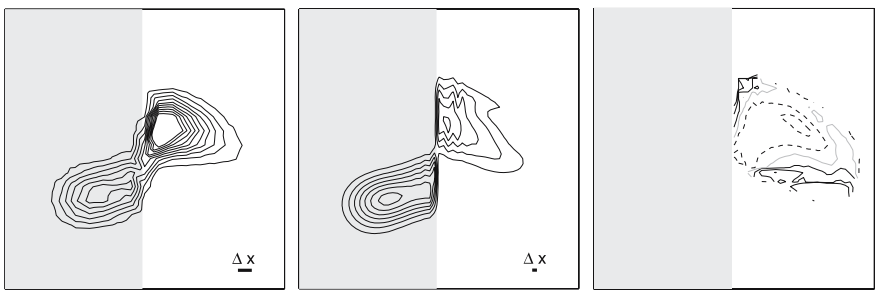

Figure 13. As Figure 7, only for the idealized topography.

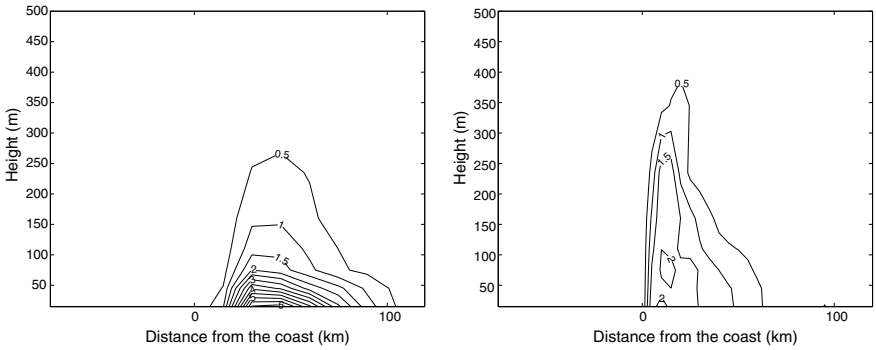

Figure 14. Vertical cross-section of the tracer concentration in $\mu g/m^3$ above the grid point with the highest concentration at the sea surface; 15 km model (left) and 5 km model (right). Contour spacing is $0.5\,\mu g/m^3$.

at the grid point with the highest tracer concentration at the sea surface. Two completely different regimes are found: in the 15 km simulation, most of the tracer is concentrated at low levels where it is available for deposition. In the 5 km run the tracer is advected towards the coast where it is partly entrained into the rising air in the convergence zone, and partly deposited to the sea surface. The same also happens around two hours later in the 15 km run, but then the amount of tracer is already significantly reduced at the lowest levels so that the deposition along the coast is much smaller than in the 5 km simulation. This experiment thus demonstrates that the three-dimensional tracer distribution is the main factor which determines where and to what extent the dry deposition would take place. Consequently, the surface wind stress, direct proxy for the deposition velocity, is of secondary importance. But, as we have seen, the regions of the increased wind stress also occur as the consequence of the same dynamics as the one that drives the advection of the tracer gas. Furthermore, both are strongly affected by the horizontal model resolution.

6. Conclusions

When coastal dynamics, in this paper limited to sea-breeze, plays important role, the horizontal resolution of a meteorological model directly influences the resulting forecast. Here it has been shown that the model results obtained with 15 km and 5 km grid spacing significantly differ from each other concerning the modelling of the dry deposition. In the presented case, the main issue is the inability of the 15 km simulation to correctly represent the onset and development of the sea-breeze. The idealized experiment has confirmed that this is strictly related to the model resolution, i.e. the discrete representation of the continuous space. The horizontal

pressure gradient is determining the development of the sea-breeze circulation. This gradient depends, given a certain temperature contrast, directly on the model grid spacing.

One of the underlying motives for this study was whether the dry deposition can alone trigger algae blooms. Based on the findings we cannot definitively answer this question. We can however state that the opposite cannot be claimed on the basis of a low-resolution model. Also Asman [17] recognizes 5 km grid spacing as a limit of possibly accurate modelling of the transport and deposition of ammonia. This is particularly true since a high deposition event is needed for triggering a bloom, rather than a long-term average, which is more likely to be correct even in a low resolution model. Therefore, it might be concluded that local phenomena, algal blooms as an example, cannot be successfully and accurately predicted by numerical modelling alone unless the transport and deposition model runs at high enough resolution. When low-resolution models are used for this purpose, their results must be interpreted carefully and properly, recognizing not only the large sub-grid variations in the surface layer, but also the possibility of the complete lack of important dynamical features in the atmospheric flow.

Acknowledgements

We appreciate the constructive comments of the two reviewers. This work was supported by the EU V Framework Programme EVK3-1999-00014–MEAD (Marine Effects of Atmospheric Deposition).

References

1. Dundas, I., Johannessen, O.M., Berge, G. and Heimdal B.: 1988, Toxic algal bloom in Scandinavian waters, May–June 1988. *Oceanography*, April issue, 9–14.
2. MEAD: 2003, *Marine Effects of Atmospheric Deposition, EVK3-CT-1999-00014, Final Report to the European Commission.* 73 pp.
3. Singles, R., Sutton, M.A. and Weston K.J.: 1998, A multi-layer model to describe the atmospheric transport and deposition of ammonia in Great Britain. *Atmos. Environ.* **32**, 393–399.
4. Asman, W.A.H.: 1998, Factors influencing local dry deposition of gases with special reference to ammonia. *Atmos. Environ.* **32**, 415–421.
5. Hasager, C.B., Carstensen, J., Ellermann, T., Gustafson, B.G., Hertel, O., Johnsson, M., Markager, S. and Ambelas Skjøth, C.: 2003, On extreme atmospheric and marine nitrogen fluxes and chlorophyll-a levels in the Kattegat strait. *Atmos. Chem. Phys.* **3**, 797–812.
6. Schlünzen, K. and Pahl S.: 1992, Modification of dry deposition in a developing sea-breeze circulation – a numerical case study. *Atmos. Environ.* **26A**, 51–61.
7. Žagar, M., Svensson, G. and Tjernström, M.: 2003, Method for determining the variability of the surface turbulent momentum flux seaward of the coast. *J. Appl. Met.* **42**, 291–307.

8. Žagar, M. and Rakovec, J.: 1999, Small-scale surface wind prediction using dynamic adaptation. *Tellus*, **51**, 489–504.
9. Hodur, R.M.: 1997, The Naval Research Laboratory's Coupled Ocean/Atmosphere Mesoscale Prediction System (COAMPS). *Mon. Wea. Rev.* **125**, 1414–1430.
10. Mellor, G. and Yamada, T.: 1974, A hierarchy of turbulence closure models for planetary boundary layers. *J. Atmos. Sci.* **31**, 1791–1806.
11. Rutledge, S.A. and Hobbs, P.V.: 1983, The mesoscale and microscale structure of organization of clouds and precipitation in midlatitude cyclones. VIII: A model for the "seeder-feeder" process in warm-frontal rainbands. *J. Atmos. Sci.* **40**, 1185–1206.
12. Kain, J.S. and Fritsch, J.M.: 1993, Convective parameterization for mesoscale models: The Kain-Fritsch scheme. *The Representation of Cumulus Convection in Numerical Models, Meteor. Monogr.*, No. 46. Amer. Meteor. Soc., 165–170.
13. Harshvardhan, R., Davies, D., Randall and Corsetti, T.: 1987, A fast radiation parameterization for atmospheric circulation models. *J. Geophys. Res.* **92**, 1009–1015.
14. Davies, H.C.: 1976, A lateral boundary formulation for multi-level prediction models. *Quart. J. Roy. Meteor. Soc.* **102**, 405–418.
15. Bott, A.: 1989, A positive definite advection scheme obtained by nonlinear renormalization of the advective fluxes. *Mon. Wea. Rev.* **117**, 1006–1015.
16. Bott, A.: 1992, Monotone flux limitation in the area-preserving flux-form advection algorithm. *Mon. Wea. Rev.* **120**, 2592–2602.
17. Asman, W.A.H.: 2001, Modelling the atmospheric transport and deposition of ammonia and ammonium: An overview with special reference to Denmark. *Atmos. Environ.* **35**, 1969–1983.
18. Baer, M. and Nester, K.: 1992, Parametrization of trace gas dry deposition velocities for a regional mesoscale diffusion model. *Ann. Geophysic.* **10**, 912–923.